05

Emission linewidth and α-factor of 1.55 μm-range vertical-cavity surface-emitting lasers based on InGaAs/InGaAlAs quantum wells

© S.A. Blokhin[1], Ya.N. Kovach[1,2], M.A. Bobrov[1], A.A. Blokhin[1], N.A. Maleev[1], A.G. Kuzmenkov[1], A.V. Babichev[2], I.I. Novikov[2], L.Ya. Karachinsky[2], E.S. Kolodeznyi[2], K.O. Voropaev[3], A.V. Kulikov[2], A.Yu. Egorov[4], V.M. Ustinov[1]

[1] Ioffe Institute, St. Petersburg, Russia
[2] ITMO University, St. Petersburg, Russia
[3] OAO OKB-Planeta, Veliky Novgorod, Russia
[4] Connector Optics LLC, St. Petersburg, Russia

e-mail: blokh@mail.ioffe.ru

Received June 29, 2023
Revised August 28, 2023
Accepted August 29, 2023

The emission linewidth of single-mode vertical-cavity surface-emitting lasers with an active region based on strained InGaAs/InGaAlAs quantum wells in the spectral range of 1.55 μm was studied. The removal of degeneracy in polarization of the fundamental mode (splitting of the resonance wavelength) and polarization switching (type I) associated with the transition from lasing via the short-wavelength mode to lasing via the long-wavelength one were observed. As the output optical power increased, the emission linewidth dropped to $\sim$ 30 MHz for both orthogonally polarized modes and was limited by the residual linewidth. The value of the α-factor was estimated: for the short-wavelength mode it reached 5, while for the long-wavelength mode it increased to $\sim$ 9. At an output optical power of more than 1 mW, the emission line broadening is observed, which can be associated with a gain saturation and the increased α-factor caused by a strong self-heating of the investigated laser.

Keywords: VCSEL, polarization, linewidth, α-factor.

DOI: 10.61011/EOS.2023.08.57287.5369-23

In recent years, the interest in the problems of developing long-wavelength (more than 1.2 μm) vertical-cavity surface-emitting lasers (VCSEL) has increased again [1–3]. This type of lasers is of interest not only for the development of gas sensors and systems of object recognition at a distance [4], but also for the development of a new generation of high-speed optical interconnects, including the use of spatial-division multiplexing technology [5], as well as integration with photonic integrated circuits [6]. Promising options for developing long-wavelength VCSELs for large-scale production are the hybrid integration of an effective active area based on the InAlGaAs/InP system and distributed Bragg reflectors (DBR), which provide the optimal combination of sufficient thermal conductivity and high reflectivity [7]. Two approaches can be distinguished here that have demonstrated their effectiveness for development of VCSELs in a spectral range of 1.3/1.55 μm: the use of dielectric DBRs based on CaF_2/ZnS or AlF_3/ZnS materials that have a high contrast of refraction indices [5,6,8,9] (hybrid-integrated VCSELs or HI-VCSELs), and the wafer fusion technology that allows the use of DBR advantages in the AlGaAs/GaAs system materials [1,2,10,11] (wafer-fused VCSELs or WF-VCSELs).

Although the spectral linewidth is an important parameter for classical fiber-optic communications and coherent data transmission, in the case of long-wavelength VCSELs, only a few studies can be identified that address this issue. Thus, the linewidth and the spectral line broadening factor, also known as Henry factor or α-factor, have been quite well studied for HI-VCSELs [12,13] and monolithic VCSEL [14] based on InAlGaAs quantum wells (QW) in a spectral range of 1.55 μm.

This study presents the results of investigating the linewidth and α-factor of single-mode WF-VCSELs based on InGaAs QWs in a spectral range of 1.55 μm.

The WF-VCSEL under study is designed as a vertical InAlGaAsP microcavity confined by AlGaAs/GaAs semiconductor DBRs, in which charge carriers are injected through the *n*-InP intracavity contact layers and the n+/p+-InAlGaAs tunnel junction (Fig. 1). The active region consists of seven strained InGaAs QWs (the lattice mismatch parameter is $\sim$ 1.4%) separated by InAlGaAs barrier layers, which are lattice-matched with the InP substrate. Layer doping profiles are optimized to minimize the absorption on free carriers. Optical and current confinments in the transverse direction are implemented within the concept of buried tunnel junction (BTJ) [15] with the choice of the BTJ mesa diameter and the etching depth of the tunnel junction layers to ensure single-mode lasing depending on the degree of planarization of the surface relief buried under an intracavity contact layer [16]. The active region is placed at the antinode of the longitudinal distribution of electromagnetic field of the fundamental mode, and the heavily doped layers are located at the nodes. Details of

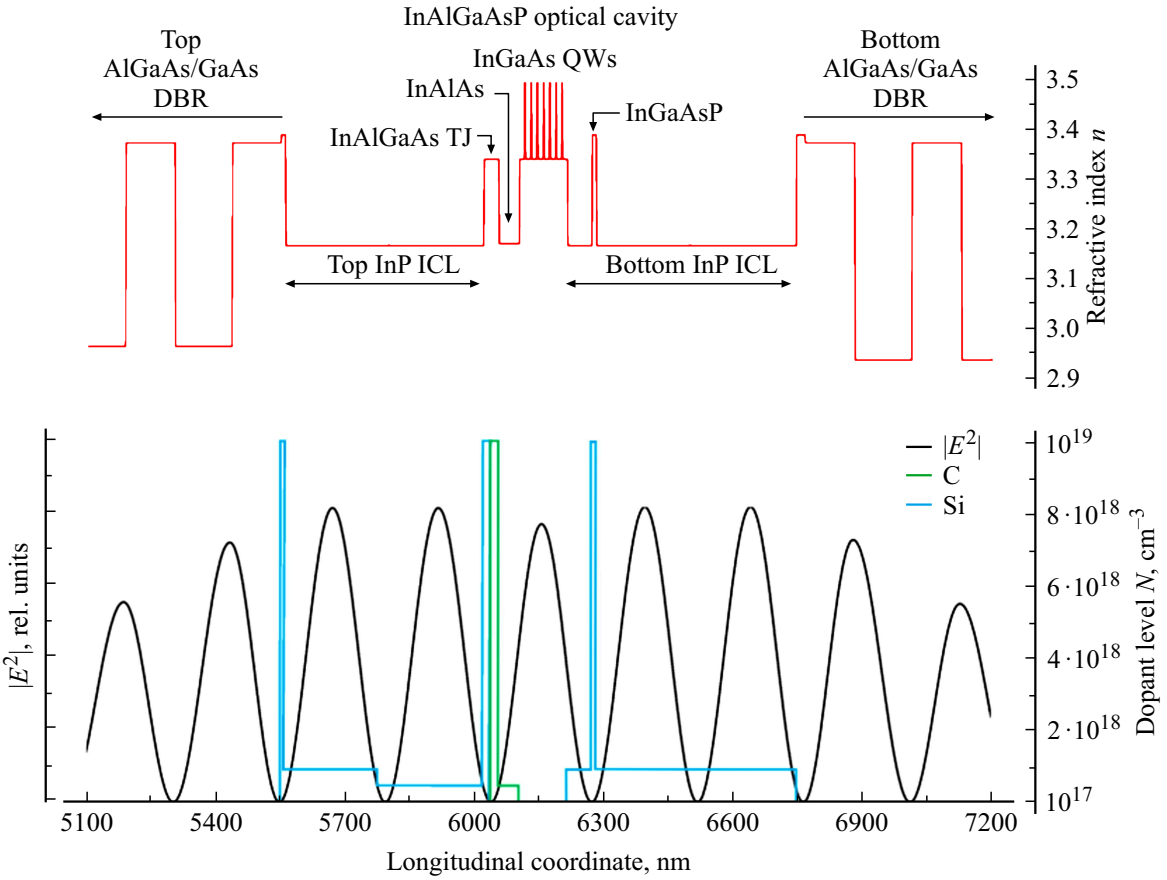

Figure 1. Longitudinal profiles of the distribution of refraction index n, the intensity of electromagnetic field of the fundamental mode $|E^2|$ and the doping level N along the optical microcavity. Legend: DBR — distributed Bragg reflector, ICL — intracavity contact layer, TJ — tunnel junction, QWs — quantum wells.

the WF-VCSEL heterostructure design and features of its formation, as well as features of the manufacturing WF-VCSEL chips, are given in [17]. Individual WF-VCSEL chips with a BTJ mesa diameter of 7 μm were mounted in microwave packeges with a fiber-optic outlet based on SMF-28 fiber (hereinafter referred to as the WF-VCSEL module); more details of the assembly design can be found in [18].

Fig. 2, *a* shows static characteristics of the WF-VCSEL module under study. The device demonstrates lasing with a threshold current of less than 1.3 mA and a maximum differential efficiency of more than 0.16 W/A. At currents above 10 mA, the self-heating effect manifestation begins, which ultimately limits the maximum output optical power at a level of 1.8 mW. It should be noted that the slope efficiency shows an anomalous behavior (Fig. 2, *b*): above the lasing threshold, there is first an increase in the differential efficiency with increasing current, which is accompanied by an abrupt change in the differential resistance (section A), followed by saturation (section B) and a drop in the differential efficiency due to thermal effects (section C).

Such behavior is usually associated with a drastical change in the mode composition of the lasing emission [19]. However, the analysis of the laser emission spectra revealed only the removal of the degeneracy of the fundamental mode in polarization (inset in Fig. 3, *a*) and the appearance of spectral splitting between two orthogonally polarized modes (~ 20 GHz) caused by the asymmetry of the BTJ buried mesa (Fig. 3, *b*) and the elasto-optical effect [20,21]. It should be noted that after dividing the wafer into individual WF-VCSEL chips, a decrease in the splitting is observed, which can be associated with a decrease in mechanical stresses arising after double wafer fusion. According to the data presented in Fig. 1, 2, the lasing begins via a shorter-wavelength fundamental mode (SW) with linear polarization along the crystallographic direction corresponding to the short axis of the BTJ mesa (section A), however, then an increase in the emission intensity of the longer-wavelength fundamental mode (LW) is observed resulting in a drop in the side-mode suppression ratio (SMSR). The appearance of abrupt changes in the dependences of the slope efficiency and differential resistance in section A (Fig. 2, *b*) corresponds to the lasing via two modes, when the SMSR coefficient is close to zero (Fig. 3, *a*). A further increase in the operating current leads to switching of the lasing to predominantly via the LW mode with a linear polarization along the crystallographic direction corresponding to the long axis of the BTJ mesa, and an SMSR of more than 30 dB (sections B–C). In this case,

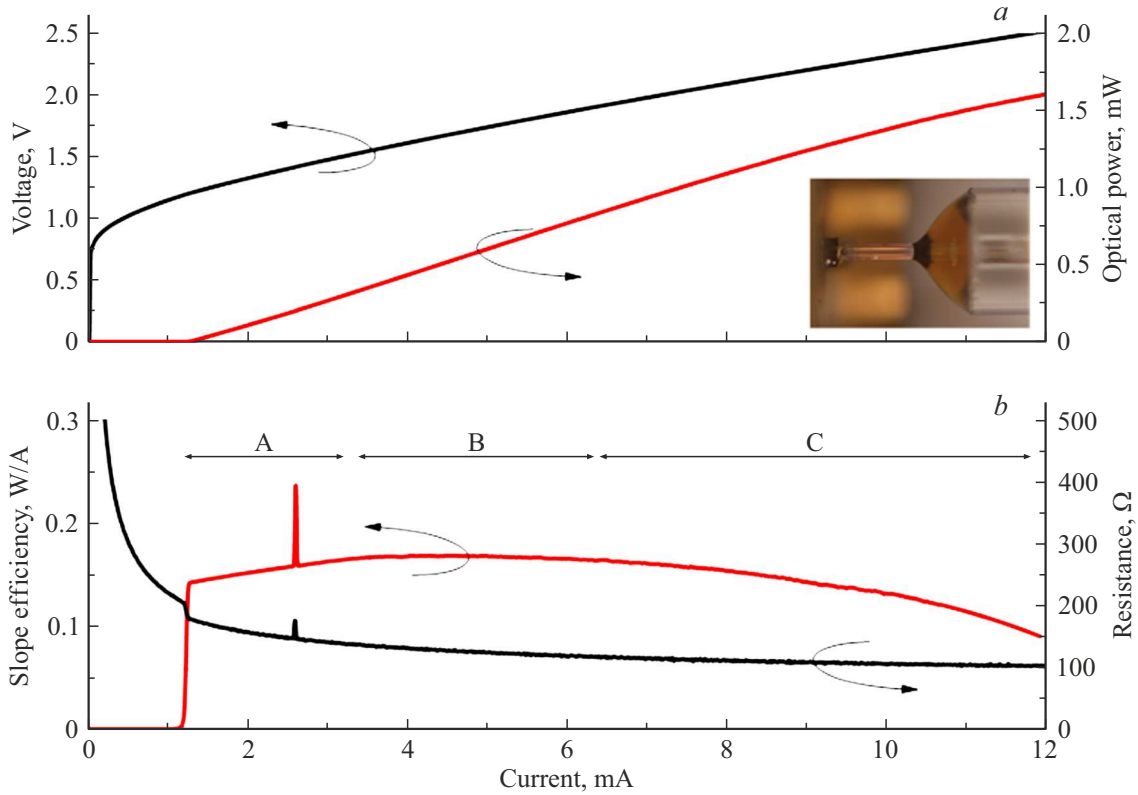

Figure 2. (*a*) Voltage-current curve (black line) and light-current curve (red line); the inset shows a specific implementation of the fiber-to-laser coupling. (*b*) Dependences of differential resistance (black line) and differential efficiency (red line) on the operating current.

the orthogonal polarization suppression ratio (OPSR) does not exceed 10 dB in both modes, which is due to the large contribution of spontaneous emission in the arrangement used for emission the coupling into the single-mode fiber (a conical microlens formed at the end of the SMF-28 fiber with an input efficiency of more than 40%, insert in Fig. 2, *a*). The observed switching of polarization from the short-wavelength mode (SW) to the long-wavelength mode (LW) (the so-called type I) is associated with a change in the spectral mismatch of the mode wavelength relative to the maximum of the gain spectrum and/or a drop in the material gain of the active region with a change in the internal temperature of the laser (self-heating) [22]. Thus, the detected anomalous behavior of the slope efficiency in the single-mode lasing is apparently due to the imperfect coupling of the fiber with the VCSEL chip, because the asymmetry of the optical confinment leads to a modification of the shape of orthogonally polarized modes and, as a consequence, to a difference in the near and far field patterns.

Fig. 4 shows the results of measuring the WF-VCSEL emission linewidth using a Thorlabs SA30-144 scanning Fabry-Perot interferometer. To suppress the noise in the power supply circuit, a chemical source was used, and to attenuate the effects associated with optical feedback, a Thorlabs IO-H-1550APC fiber optical isolator with an isolation coefficient of 29 dB was installed at the output of the WF-VCSEL. A Thorlabs LPNIR100 optical polarizer with an extinction coefficient of 40 dB was also introduced into the optical configuration for selecting the modes with orthogonal polarization. As the output optical power increases, which is indicated here taking into account the correction for the actual efficiency of the coupling the WF-VCSEL emission into the single-mode fiber, the classical behavior is first observed: a decrease in the linewidth of the WF-VCSEL emission at a rate of ~ 3.5 MHz·mW to ~ 30 MHz with an output optical power of ~ 0.37 mW. Then, there is an abrupt increase in the linewidth to 45–50 MHz associated with the switching of lasing to the long-wavelength mode (section B in Fig. 2), and a repeated sharp drop in the linewidth at a rate of ~ 11 MHz·mW to ~ 30 MHz (with an output optical power of ~ 1.15 mW). In this case, the residual linewidth of the WF-VCSEL for both orthogonally polarized modes are comparable (20–25 MHz), which can be explained by a common source of noise (for example, flicker noise). The obtained data correlates well with the data for HI-VCSEL based on InAlGaAs QWs at a comparable output optical power [12].

The magnitude of the α factor can be estimated on the linear portion of the dependence of the emission linewidth $\Delta\nu_L$ on the output optical power P using the modified Schawlow-Townes expression in a way similar to

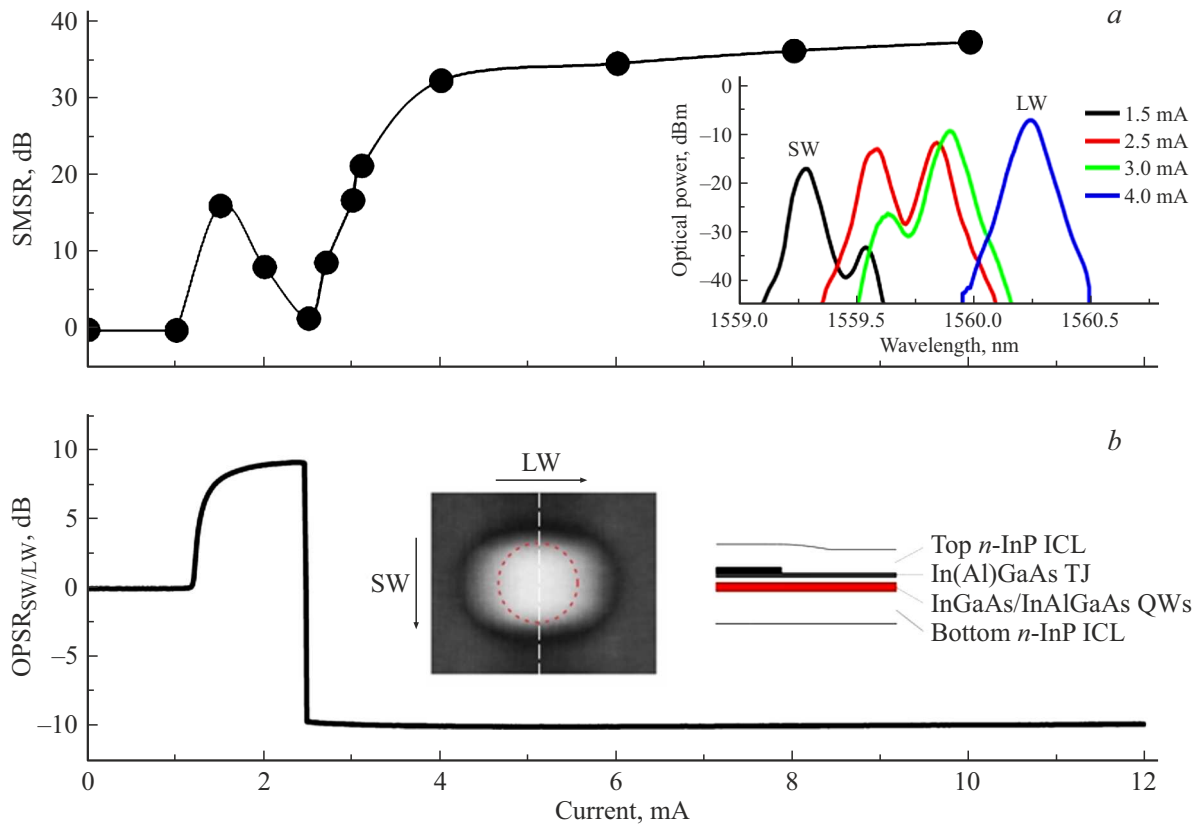

Figure 3. (*a*) Dependence of the side-mode suppression ratio (SMSR) (taking into account the removal of degeneracy of the fundamental mode) on the pump current; inset: lasing spectra. (*b*) Dependence of the orthogonal polarization suppression ratio (OPSR) on the operating current; the inset shows a schematic cross-sectional image and an image of the BTJ mesa surface before wafer fusion, obtained using atomic force microscopy.

that described in [12,13]:

$$\Delta\nu_L = \Delta\nu_o + \frac{qn_{sp}\eta_{SE}\upsilon_g^2(T_m + A_{int})^2}{4\pi PF}(1+\alpha^2),$$

where η_{SE} is slope efficiency, q is electron charge, F is fraction of optical power through the upper DBR, υ_g is group velocity ($\sim 10^{10}$ cm/s), T_m is mirror loss, A_{int} is internal optical loss, n_{sp} is population inversion factor. The mirror loss can be calculated from the value of η_{SE} using the data from the estimate of internal optical loss and the efficiency of current injection for a given type of VCSEL. The population inversion factor can vary in a wide range and depends on the threshold gain [22]. The experimental studies of long-wavelength WF-VCSEL with an active area based on InGaAsP QW used the value of $n_{sp} = 1.1$ [23], and for the first HI-VCSELs based on InAlGaAs QW the values of $n_{sp} = 1.6-2$ [12,13] were used. Assuming $n_{sp} = 1.5$, the α-factor can be estimated as ~ 5 for the short-wavelength fundamental mode, which correlates well with the data for a monolithic VCSEL [24] and HI-VCSEL [25] based on InAlGaAs QW. At the same time, for the long-wavelength fundamental mode, estimates give a higher value of the α-factor: ~ 9. On one hand, the authors of [14] did not reveal a significant difference in the magnitude of α between orthogonally polarized fundamental modes in a monolithic VCSEL based on InAlGaAs QW. On the other hand, the authors of [26,27] theoretically predicted the variation of the α-factor in the presence of anisotropic deformation in the active region. The higher value of the α-factor for the long-wavelength mode is apparently due to a drop in the differential gain with increasing charge carrier concentration in the microcavity [25].

However, at relatively high levels of the output optical power (more than 1.5 mW), an anomalous line broadening is observed (Fig. 4, *a*), which can be associated with both laser self-heating effects and non-linearity of the gain at a high density of charge carriers and photons in the microcavity [13,14]. In the case of VCSEL, the issue of ensuring effective heat removal from the pumped part of the active region is extremely urgent, because the thermal conductivity of the ternary and quaternary materials used in DBR is significantly lower than that for binary compounds. According to the analysis of lasing spectra, the shift of the resonant wavelength of the devices under study with increasing dissipated electrical power $\partial\lambda/\partial P_{\text{diss}}$ achieves ~ 0.15 nm/mW, and the shift of the resonant wavelength with increasing temperature $\partial\lambda/\partial T$ amounted to ~ 0.08 nm/K (inset in Fig. 4, *b*). It

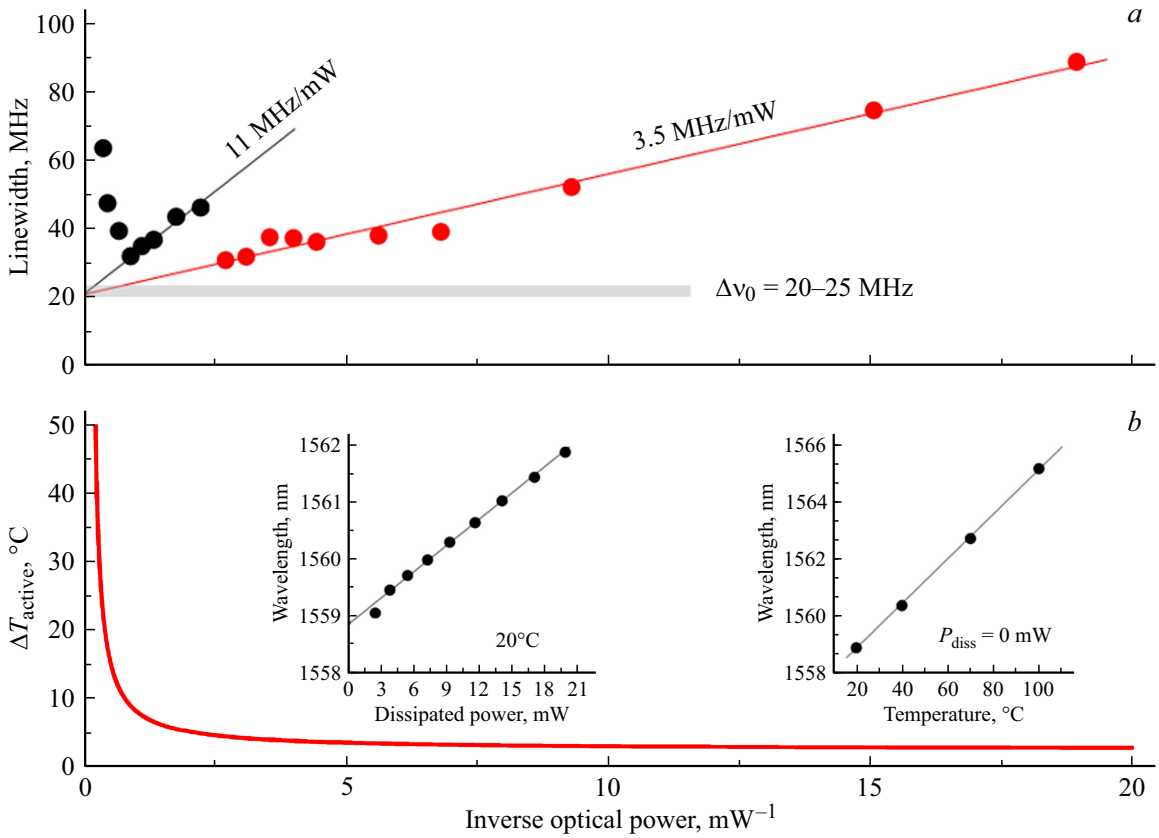

Figure 4. (a) Dependence of the emission linewidth on the reciprocal of the output optical power for two orthogonal polarizations. (b) Dependence of the change in the internal temperature of the laser ΔT_{act} on the reciprocal value of the output optical power; the insets show the wavelength shift with dissipated electrical power at 20° and the temperature shift of the cold cavity wavelength (the dissipated electrical power is 0 mW).

should be noted that for an adequate assessment of the temperature shift $\partial\lambda/\partial T$, we used the approximation of the dependences $\lambda(P_{diss})$ to the value of the dissipated electrical power $P_{diss} = 0$ (the cold microcavity mode) measured at different temperatures. Fig. 4, b shows the internal temperature of WF-VCSEL calculated by the following formula: $\Delta T_{act} = P_{diss} \cdot (\partial\lambda/\partial P_{diss})/(\partial\lambda/\partial T)$. It can be seen that even with an output optical power of more than 1 mW, a rapid increase in the internal temperature begins, which correlates with section C on the light-current curve of the devices. As a result, strong self-heating of the laser leads to gain saturation and an increase in the α-factor, which ultimately leads to a broadening of the spectral line of the WF-VCSEL emission, despite a further increase in the output optical power [13,14].

This study has analyzed the static, spectral, and polarization characteristics of a single-mode WF-VCSEL with a spectral range of 1.55 μm and with an active region based on strained InGaAs/InAlGaAs QWs. It was found that the lasing starts via a shorter-wavelength fundamental mode, however, then switches to a longer-wavelength fundamental mode with an orthogonal polarization. As the output optical power increases, the laser emission linewidth first decreases to $\sim$ 30 MHz (at 0.37 mW). With a further increase in optical power, the polarization switches resulting in an abrupt increase in the emission linewidth, which again drops to $\sim$ 30 MHz (at 1.15 mW). With a subsequent increase in the output optical power, line broadening is observed due to thermal effects. Estimates of the broadening factor of the emission spectral line showed that there is a significant difference in the values of the α-factor for short-wavelength and orthogonally polarized long-wavelength optical modes. This behavior most likely due to a drop in the differential gain with increasing charge carrier concentration in the WF-VCSEL microcavity.

Funding

The work of the group of authors from the ITMO University has been carried out with the support from the „Advanced Engineering Schools“ federal project as related to the study of optical spectra, as well as with the support of the Ministry of Science and Higher Education of the Russian Federation, the research project № 2019-1442, as related to a number of studies of static and polarization characteristics.

Conflict of interest

The authors declare that they have no conflict of interest.

References

[1] A. Babichev, S. Blokhin, A. Gladyshev et al. IEEE Photonics Technol. Lett., **35** (6), 297 (2023). DOI: 10.1109/LPT.2023.3241001

[2] S.A. Blokhin, A.V. Babichev, A.G. Gladyshev et al. IEEE J. Quant. Electron., **58** (2), 2400115 (2022). DOI: 10.1109/jqe.2022.3141418

[3] M. Gebski, D. Dontsova, N. Haghighi et. al. OSA Continuum, **3** (7), 1952 (2020). DOI: 10.1364/osac.396242

[4] B.D. Padullaparthi, J. Tatum, K. Iga, *VCSEL Industry: Communication and Sensing, The ComSoc Guides to Communications Technologie* (Wiley-IEEE Press, Piscataway, NJ., USA, 2022). ISBN: 9781119782216

[5] Z. Ruan, Y. Zhu, P. Chen et al. J. Lightwave Technol., **38**, 5100 (2020). DOI: 10.1109/jlt.2020.2999526

[6] L. Zhang, J. Van Kerrebrouck, R. Lin et al. J. Lightwave Technol., **37** (2), 380 (2019). DOI: 10.1109/JLT.2018.2851746

[7] A. Babichev, S. Blokhin, E. Kolodeznyi et al. Photonics, **10** (3), 268 (2023). DOI: 10.3390/photonics10030268

[8] S. Spiga, W. Soenen, A. Andrejew et al. J. Lightwave Technol., **35** (4), 727 (2017). DOI: 10.1109/JLT.2016.2597870

[9] S. Spiga, D. Schoke, A. Andrejew et al. J. Lightwave Technol., **35** (15), 3130 (2017). DOI: 10.1109/jlt.2017.2660444

[10] D. Ellafi, V. Iakovlev, A. Sirbu et al. Opt. Express, **22** (26), 32180 (2014). DOI: 10.1364/OE.22.032180

[11] A. Sirbu, G. Suruceanu, V. Iakovlev et al. IEEE Phot. Technol. Lett., **25** (16), 1555 (2013). DOI: 10.1109/LPT.2013.2271041

[12] A. Bacou, A. Rissons, J.-C. Mollier. Proc. SPIE, **6908**, 69080F (2008). DOI: 10.1117/12.763054

[13] R. Shau, H. Halbritter, F. Riemenschneider et al. Electron. Lett., **39** (24), 1728 (2003). DOI: 10.1049/el:20031143

[14] N.A. Khan, K. Schires, A. Hurtado et al. IEEE J. Quantum Electron., **49** (11), 990 (2013). DOI: 10.1109/jqe.2013.2282759

[15] M. Ortsiefer, R. Shau, G. Böhm et al. Appl. Phys. Lett., **76** (16), 2179 (2000). DOI: 10.1063/1.126290

[16] S.A. Blokhin, M.A. Bobrov, A.A. Blokhin et al. Tech. Phys. Lett., **48** (14), 46 (2022). DOI: 10.21883/TPL.2022.14.55117.18942

[17] S.A. Blokhin, A.V. Babichev, L.Ya. Karachinsky et al., Kvant. elektron., **52** (10), 878 (2022) (in Russian).

[18] S.A. Blokhin, A.V. Babichev, L.Ya. Karachinsky et al. J. Opt. Technol., **89** (11), 681 (2022). DOI: 10.1364/JOT.89.000681

[19] S.A. Blokhin, M.A. Bobrov, N.A. Maleev et al. Appl. Phys. Lett., **105** (6), 061104 (2014). DOI: 10.1063/1.4892885

[20] N. Volet, V. Iakovlev, A. Sirbu et al. Proc. SPIE, **8432**, 84320B (2012). DOI: 10.1117/12.922075

[21] L. Yu, Y.H. Chen, C.Y. Jiang et al. J. Appl. Phys., **111** (4), 043109 (2012). DOI: 10.1063/1.3682648

[22] L.A. Coldren, S.W. Corzine, M.L. Mašanović. *Diode Lasers and Photonic Integrated Circuits* (John Wiley & Sons, Hoboken, NJ., USA, 2012). ISBN: 9780470484128

[23] N.M. Margalit, J. Piprek, S. Zhang et al. IEEE J. Sel. Top. Quant. Electron., **3** (2), 359 (1997). DOI: 10.1109/2944.605679

[24] N.A. Khan, T. Mahmood. J. Mod. Opt., **67** (16), 1334 (2020). DOI: 10.1080/09500340.2020.1845406

[25] H. Halbritter, R. Shau, F. Riemenschneider et al. Electron. Lett., **40** (20), 1266 (2004). DOI: 10.1049/el:20040173

[26] D. Burak, J.V. Moloney, R. Binder. IEEE J. Quant. Electron., **36** (8), 956 (2000). DOI: 10.1109/3.853556

[27] G. Van der Sande, J. Danckaert, I. Veretennicoff et al. Phys. Rev. A, **71** (6), 063801 (2005). DOI: 10.1103/PhysRevA.71.063801

Translated by Y.Alekseev